Int J Adv Manuf Technol (2001) 18:79–88

The International Journal of
Advanced Manufacturing Technology

Collapse Pressure and Strength Analysis of Hydroformed Circular Plates

A. H. Elkholy and O. M. Al-Hawaj

Mechanical and Industrial Engineering Department, Kuwait University, Kuwait

Hydroforming processing of sheet metal parts provides a number of advantages over conventional processes including the reduction in the number of parts, and reduction in the tooling and material costs. As a result, the technology has attracted increasing attention in many industries. However, there is still little experience available of both the process and its associated stresses and deformation which limit the application of this technique. The current study has been initiated to gain a better understanding of the fundamentals of the hydroforming process and the limitations on its applicability. The study outlines the stress and deformation distributions when a circular plate is processed by a hydrostatic transverse pressure that causes the plate to deform in the axial direction. The collapse load that leads to excessive and uncontrollable deformation is also determined and a forming limit is established. Experimental verification is also carried out to establish the validity of the analytical results.

Keywords: Circular plates; Collapse pressure; Deformation; Hydroforming; Yield stress

1. Introduction

Owing to the many advantages of the hydroforming processes over conventional forming processes, such as part reduction and hence reduction in the associated tooling and material costs, the technology has attracted increasing attention in the industrial sector. The hydroforming process can form most ferrous and non-ferrous geometric shapes in a single operation. Stepped, irregular-shaped parts can be produced in a single step, rather than in the series of steps that would be required with other forming processes. This helps to minimise set-up and changeover time and eliminates an intermediate annealing process that is usually required with conventional forming operations.

Correspondence and offprint requests to: Professor A. H. Elkholy, Mechanical and Industrial Engineering Department, Kuwait University, PO Box 5969, Safat-13060, Kuwait. E-mail: kholy@kuc01.kuniv.edu.kw

Several applications in the automotive industry, where parts are processed by hydroforming, have been reported, such as an engine cradle [1], a subframe [2], and an instrument panel beam [3]. Other applications may include the production of smooth, scratchfree surfaces (lighting reflectors), cooking and serving products for the food industry and painted preformed products [4]. However, hydroforming cannot, in general, perform punching or secondary operations. When the finished part requires these operations, secondary tooling is required, or other operations must be used.

In the hydroforming process (see Fig. 1), the metal blank is placed on the forming die which can have a predetermined profile or can be just an open cavity allowing the blank to deform freely. The pressure chamber is lowered and when it is in position, the diaphragm clamps the blank to the die. The pressure chamber is then filled with hydraulic fluid and pressurised to form the part. The required pressure depends on the geometric shape, alloy type and grade, and the thickness of the blank, and usually ranges from 30 to 500 bar. After the part is formed, the chamber is decompressed, and raised, and the formed part is removed from the die.

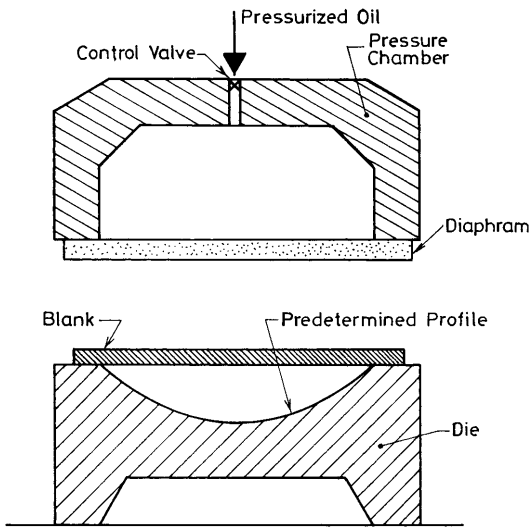

Fig. 1. Schematic view.

In the hydroforming process, the shape of the finished part is determined only by the configuration of the die and, unlike the conventional forming processes, there is no corresponding mating die. This helps to minimise the high local strains, which result in blank thinout, and the possibility of failure, either by wrinkling or rupture [5]. Therefore, the blank thickness is nearly equal to the thickness of the finished part. Moreover, tolerances can be held at a minimum, resulting in an improvement of dimensional accuracy.

Nevertheless, hydroforming has some limitations, for instance, it cannot handle high-volume production, and cannot perform secondary operations efficiently without involving secondary tooling. Therefore, it is not suited for multistage forming, nor is it appropriate for very deep drawing operations when the depth to diameter ratio exceeds 3:1.

The present paper summarises the results of hydroforming a circular plate supported at its periphery and subjected to a uniformly increasing transverse hydrostatic pressure that tends to deform the plate laterally. Both the stress and deformation distributions, as well as the oil pressure at collapse, are determined. Experimental results obtained from the literature are compared with those obtained in this study.

2. Analysis

As an initial approach, we consider first the behaviour of a circular plate, radius a and thickness h, resting on a continuous simple support around its edge and sustaining a uniformly distributed transverse load of intensity p per unit area, as shown in section in Fig. 2(*a*).

The plate is a 3D body, and the loading sets up a variety of stresses within the body which, because of the symmetry of the situation, may be classified broadly as follows:

1. Shearing stresses on concentric circular cylindrical "cuts".
2. Compressive stresses in the direction of the axis of rotational symmetry.
3. "In-plane" stresses, compressive at the upper surface and tensile stresses at the lower surface of the plate.

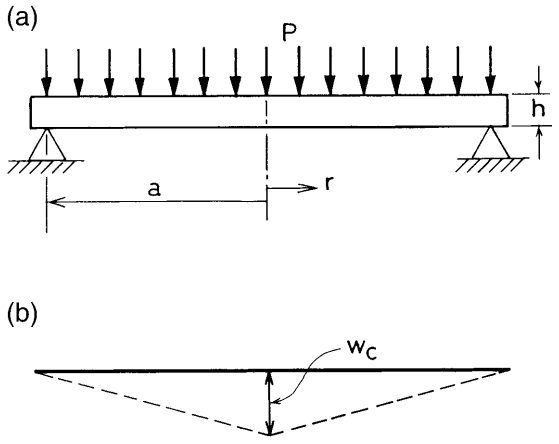

Fig. 2. A simply supported circular plate carrying a uniformly distributed transverse load (P per unit area). (*a*) Plate parameters. (*b*) Collapse mechanism.

Following traditional plate theory we seek ways of avoiding analysis of a fully 3D situation. The key to the desired simplification is the observation that for sufficiently thin plates (i.e. thickness/diameter sufficiently small) stresses in classes (1) and (2) are negligible compared to the in-plane stress (class 3). This enables us to assume that the bending strength of the elements of the plate is unaffected by the small shear (1) and pressure (2) effects, and, hence, to set up the problem as 2D in terms of the variation of bending moments over a surface.

2.1 Yield Locus for an Element of the Plate

One of our preliminary tasks is to set up a "yield locus" in a suitable bending-moment space. Figure 3 shows a typical element of the plate (defined by radial and circumferential cuts) and the resultant stresses which act upon it: those which vanish by virtue of symmetry are not indicated. The bending moments M_r and M_θ per unit length (which have the dimensions of force) are, by symmetry, principal bending moments. The shearing stress resultant Q_r is necessary for equilibrium, but, as we have argued, it does not affect the yield condition. In Fig. 3, all the resultant stresses are shown in their positive senses.

To establish the required yield locus in M_r, M_θ space we investigate the strength of an element in pure biaxial bending, as shown in Fig. 4(*a*). It is convenient for this purpose to imagine the element slit into a number of parallel thin layers, symmetrically disposed about the central surface. We can easily achieve a state of full-plastic pure biaxial bending in a pair of layers by setting the σ_r, σ_θ stress points for the two layers at diametrically opposite points on the relevant biaxial yield locus, for example C and C' in Fig. 4(*b*). If the distance of the two layers from the central surface is $\pm z$ and the thickness of the layers is δz, we have the following expressions for the corresponding contributions of bending moment:

$$\left.\begin{aligned}\delta M_r &= 2\,z\,\sigma_r^c\,\delta z\\ \delta M_\theta &= 2\,z\,\sigma_\theta^c\,\delta z\end{aligned}\right\} \tag{1}$$

where σ_r^c, σ_θ^c are the coordinates of point C.

If we now assign the stress state C to all layers above the centre surface and state C' to all layers below the centre

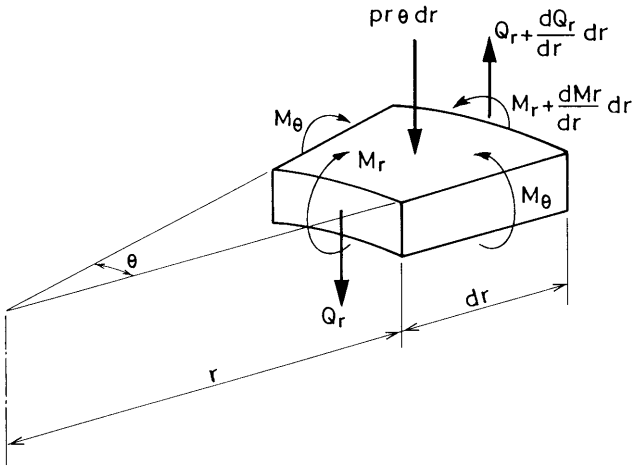

Fig. 3. Equilibrium of a small element of the plate.

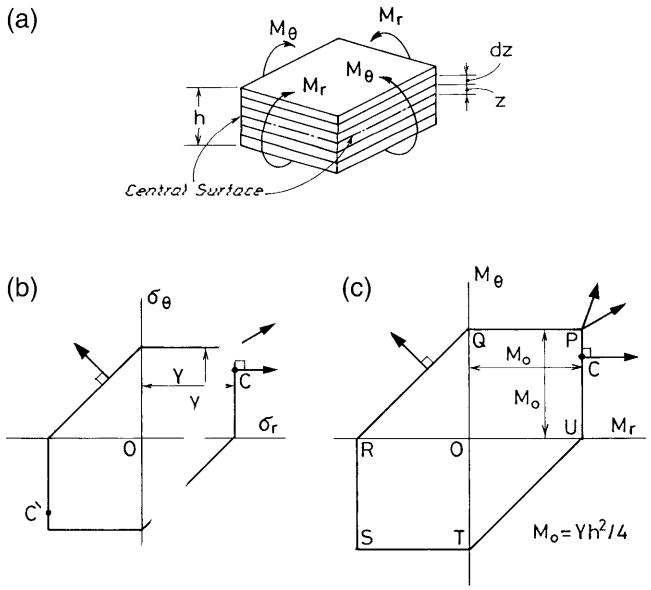

Fig. 4. Biaxial plastic bending of an element of the plate.

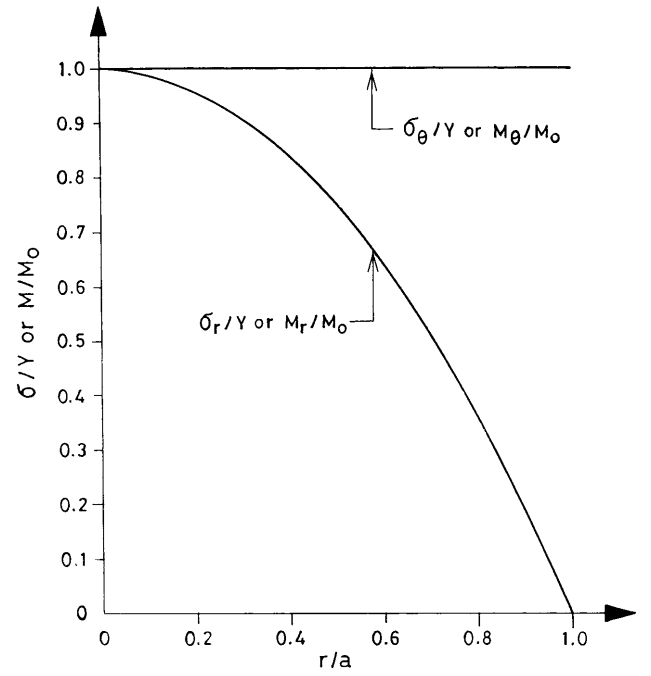

Fig. 5. The bending moment and stress distribution at collapse of a simply supported plate.

surface, we can integrate through the thickness to give the following "safe" pure bending moments:

$$\left.\begin{aligned} M_r &= \sigma_r^c\, h^2/4 \\ M_\theta &= \sigma_\theta^c\, h^2/4 \end{aligned}\right\} \tag{2}$$

The locus in the M_r, M_θ space, shown in Fig. 4(c) is similar to the yield locus in σ_r,σ_θ space. The leading dimension is M_o:

$$M_o = Y\, h^2/4 \tag{3}$$

where Y represents the yield stress of the material in simple tension (see Fig. 4(b)).

2.2 Equations of Equilibrium

We obtain the necessary equilibrium Eq. for the plate by considering the equilibrium of the small element shown in Fig. 3. Two non-trivial relationships are found by taking moments about a local circumferential axis and resolving in the direction perpendicular to the plate, respectively:

$$\frac{\mathrm{d}}{\mathrm{d}r}(rM_r) = M_\theta - rQ_r \tag{4}$$

$$\frac{\mathrm{d}}{\mathrm{d}r}(rQ_r) = pr \tag{5}$$

In the present problem, Eq. (5) may be integrated to give

$$Q_r = pr/2 \tag{6}$$

This equation may also be obtained by considering the equilibrium of a disk "cut out" at radius r. Substituting for Q_r in Eq. (4) (to eliminate the resultant stress which does not appear in the yield condition) we obtain

$$\frac{\mathrm{d}}{\mathrm{d}r}(rM_r) = M_\theta - pr^2/2 \tag{7}$$

2.3 Collapse Pressure in Simply Supported Plates

To find the collapse pressure p_c, we must satisfy the equilibrium equation (Eq. (7)) without violating the yield condition, Fig. 4(c), as well as the boundary condition corresponding to the simple support which is,

$$M_r = 0 \quad \text{at } r = a \tag{8}$$

It seems clear, intuitively, in the present problem that both M_θ and M_r will be positive throughout, and so we might guess that the M_r, M_θ "trajectory" will lie on either PQ or PU in Fig. 4(c). If we put $M_r = M_o$ (corresponding to PU) in Eq. (7), we find $M_\theta > M_o$ for positive values of p, which violates the yield condition. We, therefore, try the alternative, $M_\theta = M_o$ in Eq. (7) and integrate to give:

$$M_r = M_o - \frac{pr^2}{6} + \frac{C}{r} \tag{9}$$

C is a constant of integration. According to this equation, M_r is infinite at the centre of the plate if C is finite; we conclude from this that C must be zero, so

$$M_r = M_o - \frac{pr^2}{6} \tag{10}$$

Finally, using the boundary condition (8), we obtain

$$p_c = 6M_o/a^2 \tag{11}$$

after checking that the M_r, M_θ trajectory does not extend beyond the postulated segment PQ.

From Eqs (3) and (11), we have

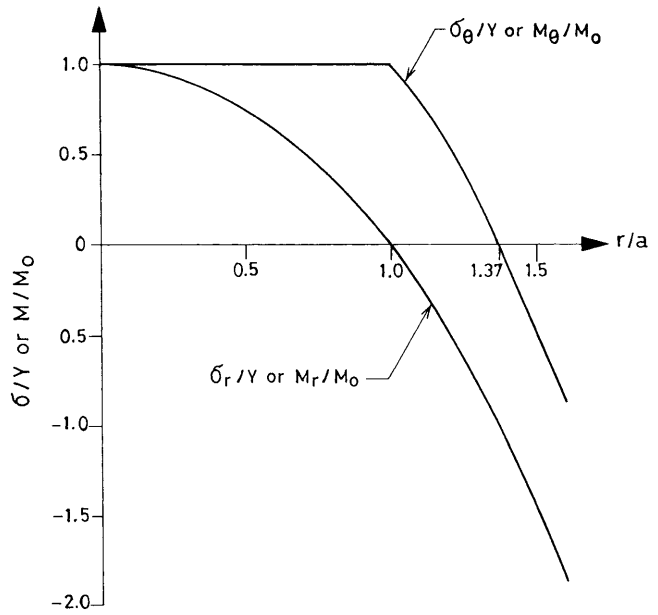

Fig. 6. Radial distribution of bending moments and stresses at collapse of a clamped-edge plate (plate radius $b = 1.37a$).

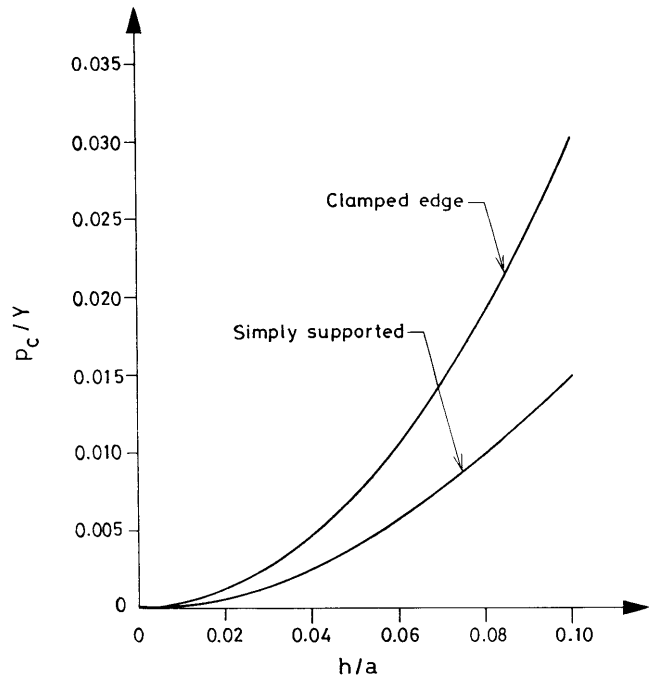

Fig. 7. Collapse pressure vs. plate thickness ratio.

$$\frac{p_c}{Y} = \frac{3}{2}\left(\frac{h}{a}\right)^2 \tag{12}$$

which determines the collapse pressure p_c as a function of the yield strength in simple tension, and the thickness to radius ratio of the plate.

2.4 Collapse Pressure in a Clamped Circular Plate

It is relatively simple to extend the analysis above to deal with a circular plate which is supported by a fully clamped edge. It is intuitively obvious that M_r will be negative at and near the clamped edge, so the M_r, M_θ trajectory PQ, Fig. 4(c), will be inadequate by itself. Now, M_r must be a continuous function of r, and so there must exist a radius within the clamped plate at which $M_r = 0$. Within this radius, conditions are exactly the same as for a simply supported plate of a smaller radius. Our best strategy, therefore, is to build on our previous work, using the value of p given by Eq. (11) and regarding a as the radius at which the M_r, M_θ trajectory changes from one edge of the yield locus to another. We shall seek a larger radius b for the clamped edge, and having found it, we shall be able to express the safe pressure to avoid collapse in terms of this radius.

Substituting for p from Eq. (11), the equilibrium equation (Eq. (7)) becomes:

$$\frac{\mathrm{d}}{\mathrm{d}r}(rM_r) = M_\theta - \frac{3M_o r^2}{a^2} \tag{13}$$

It seems clear that, for $r > a$, we shall be in the second quadrant of M_r, M_θ space, for which the equation of the yield condition is (Fig. 4(c))

$$M_\theta - M_r = M_o \tag{14}$$

To solve these two Eq. simultaneously, we first differentiate the product in Eq. (13) and obtain

$$\frac{\mathrm{d}M_r}{\mathrm{d}r} = \frac{M_\theta - M_r}{r} - \frac{3M_0 r}{a^2} \tag{15}$$

Using Eq. (14) and integrating, we have:

$$M_r = M_o \ln r - \frac{3}{2}\frac{M_o r^2}{a^2} + C \tag{16}$$

The constant of integration, C, is determined by the fact that $M_r = 0$ at $r = a$; this gives us

$$M_r = M_o = \ln (r/a) = 3/2\ M_o \left[\left(\frac{r}{a}\right)^2 - 1\right] \tag{17}$$

This Eq. is valid only if the M_r, M_θ trajectory is on QR, Fig. 4(c). It is not possible to extend the trajectory into RS, and so point R must correspond to the clamped edge, $r = b$. From Eq. (17), we find that the clamped edge is reached at $b/a \cong 1.37$. As the pressure $p = 6M_o/a^2$ is a safe pressure for a clamped plate of radius b, we obtain, finally,

$$\left.\begin{aligned} p_c &\cong 11.3\ M_o/b^2 \\ \frac{p_c}{Y} &\cong 3\left(\frac{h}{a}\right)^2 \end{aligned}\right\} \tag{18}$$

from Eq. (3). Comparing Eqs (11) and (18) we see that by clamping the edge of a uniform circular plate we almost double its collapse pressure or simply its load-carrying capacity.

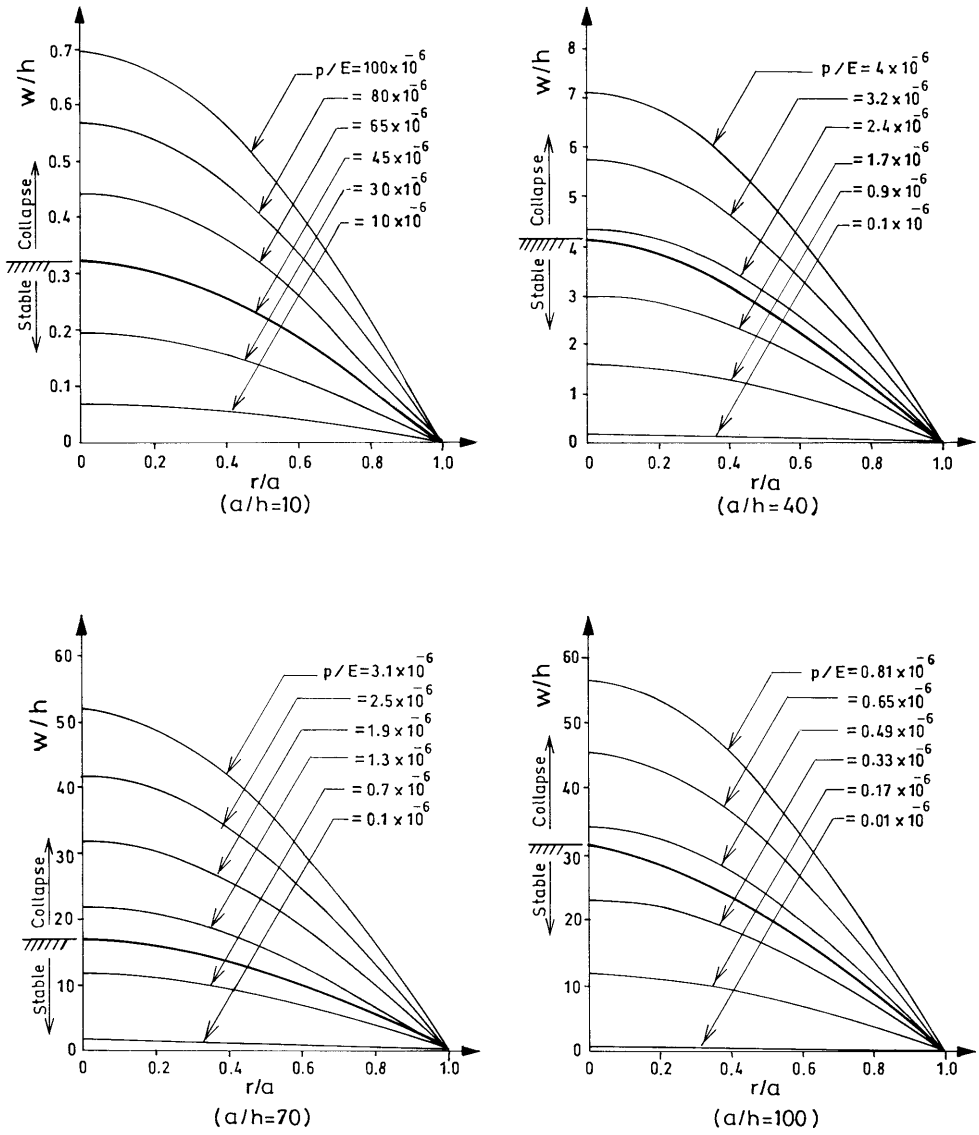

Fig. 8. Lateral deformation of simply supported plates.

2.5 Modes of Deformation

In plastic collapse analysis, we will assume that deflections are small, even in the plastic collapse mode, and the material is perfectly elastic-plastic. With these assumptions, we ignore the possible strain hardening of the material and the possible effect of membrane stresses due to large deflections. For circular plates, a possible collapse mechanism is shown in Fig. 2(*b*). This "conical mode" is a virtual displacement that appears after the collapse load is reached.

The lateral deflection w of the circular plate during the early stages of deformation is determined non-dimensionally from the following two expressions [6]:

$$\left(\frac{w}{h}\right) = \left[1 - \left(\frac{r}{a}\right)^2\right]^2 \left(\frac{a}{h}\right)^4 \frac{3P(1-\nu^2)}{16E}$$

for clamped edge case (19)

$$\left(\frac{w}{h}\right) = \frac{3P(1-\nu^2}{16E}\left(\frac{a}{h}\right)^4 \left[1 - \left(\frac{r}{a}\right)^2\right] \left[\left(\frac{5+\nu}{1+\nu}\right) - \left(\frac{r}{a}\right)^2\right] \quad (20)$$

for simply supported case

where E and ν are the Young's modulus of elasticity and Poisson's ratio, respectively. If lateral deflection is not small, it becomes necessary to account for the effect of midsurface stretching, which we have thus far ignored in the derivation of Eqs (19) and (20). The effect introduces nonlinearities, so that lateral deflection is not directly proportional to lateral load. Details of analysis appear in other publications [7–9]. For a uniformly loaded circular plate whose edge is simply supported, an approximate expression for the central deflection $w_o(r = 0)$ is given in [9] for $\nu = 0.3$ as:

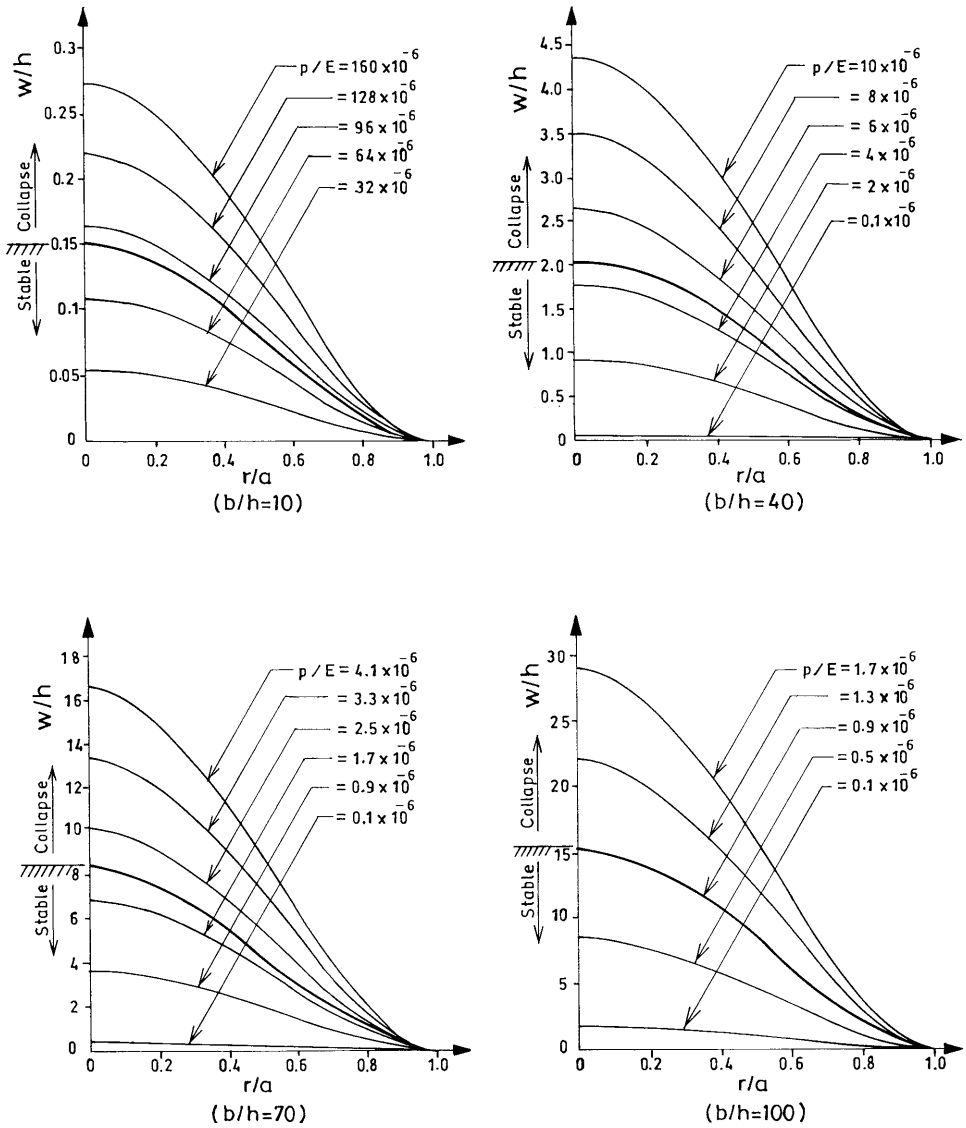

Fig. 9. Lateral deformation of clamped-edge plates.

$$\left(\frac{w_o}{h}\right) + 0.262\left(\frac{w_o}{h}\right)^3 \cong \frac{3P(1-\nu^2)}{4E}\left(\frac{a}{h}\right)^4 \tag{21}$$

When the load, dimensions, and elastic properties are prescribed, w_o/h is obtained from the equation.

3. Results and Discussion

A detailed analysis of a hydroformed circular plate processed by the effect of lateral steadily increasing static pressure is carried out in this study. Both the simply supported and clamped edge cases are investigated. It is intended to determine the distribution of bending moments as well as the stresses throughout the plate, and consequently the location of a critical zone where the plate may fail owing to excessive thinning and/or rupture is expected to take place, resulting in limiting the application of the hydroforming technique. Lateral plate deformation is also determined and an upper limit on its magnitude is established.

3.1 Bending Moment and Stress Distribution

3.1.1 Simply Supported Plates

The bending moment distribution in the radial direction at the onset of yielding M_r for a simply supported plate is determined from Eqs (10) and (11) as

$$\frac{M_r}{M_o} = 1 - \left(\frac{r}{a}\right)^2 \tag{22}$$

The bending moment in the tangential direction is, however, constant throughout the plate and is equal to the upper limit M_o, i.e.

$$\frac{M_\theta}{M_o} = 1 \tag{23}$$

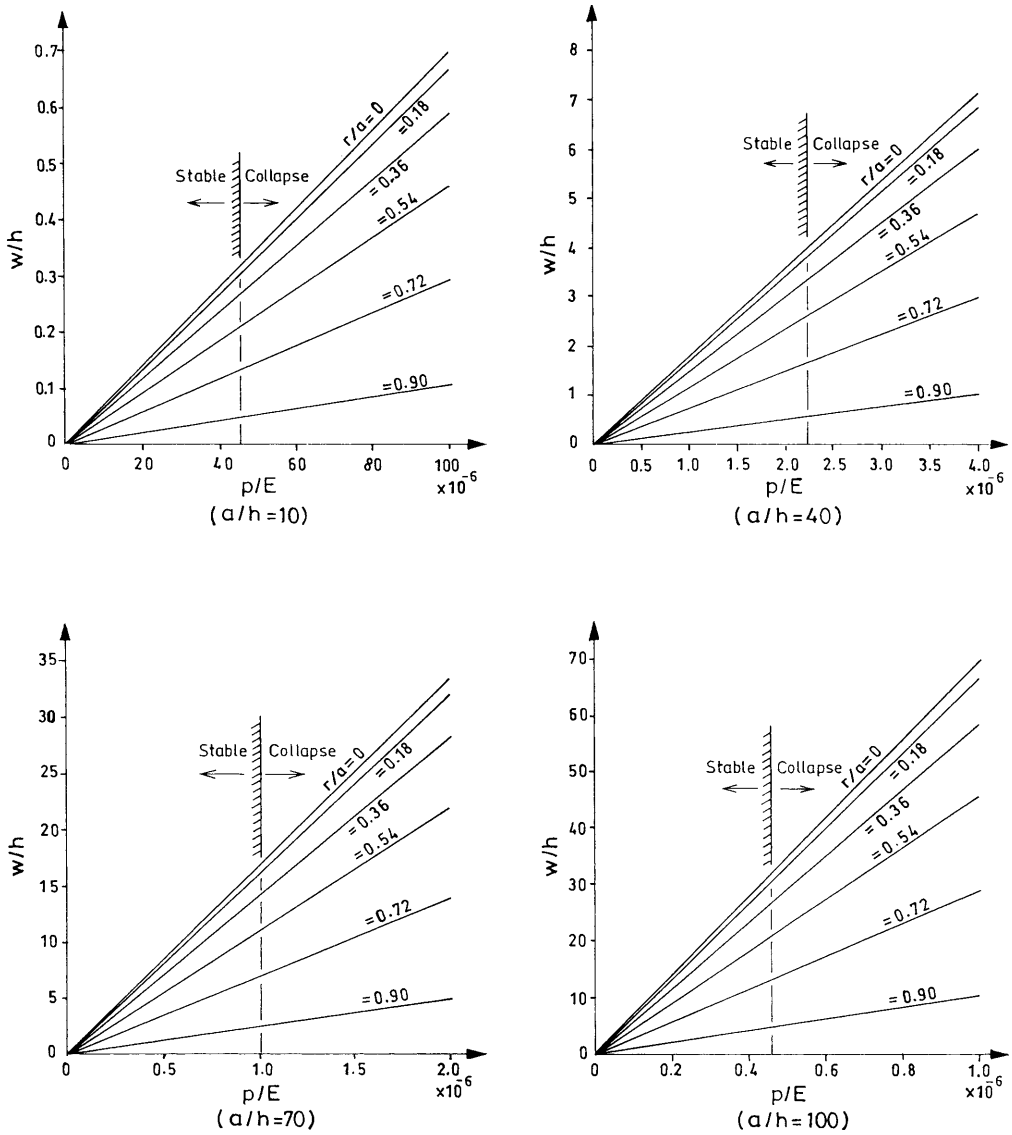

Fig. 10. Lateral deformation vs. applied pressure for simply supported plates.

The radial and tangential stresses σ_r and σ_θ, respectively, were determined from Eqs (2) and (3) and found to be similar to their bending moment counter values, i.e.

$$\left.\begin{aligned}\frac{\sigma_r}{Y} &= 1 - \left(\frac{r}{a}\right)^2 \\ \frac{\sigma_\theta}{Y} &= 1\end{aligned}\right\} \tag{24}$$

Equations (22) to (24) are plotted in Fig. 5 and maximum (critical) values are found to take place at the centre of the plate, as shown.

3.1.2 Clamped Edge Plates

The bending moment distribution is determined using the results of the simply supported plate case for positive values of M_r, and Eqs (14) and (17) for negative values of M_r. The results are presented in Fig. 6 where M_r reaches zero at $r = a$.

Both M_r and M_θ decrease in value as r/a increases beyond unity. At the plate edge ($r/a = 1.37$) the magnitude of M_r/M_o becomes negative and M_θ/M_o diminishes. Both stresses σ_r and σ_θ follow the trend of their counterparts M_r and M_θ, as shown in Fig. 6.

3.2 Collapse Pressure

The collapse pressure for simply supported plates is determined from Eq. (12), and from Eq. (18) for clamped-edge plates. It is presented in Fig. 7 for various thickness to radius ratios. The figure indicates that increasing the thickness to radius ratio tends to increase the collapse pressure and the relationship is parabolic.

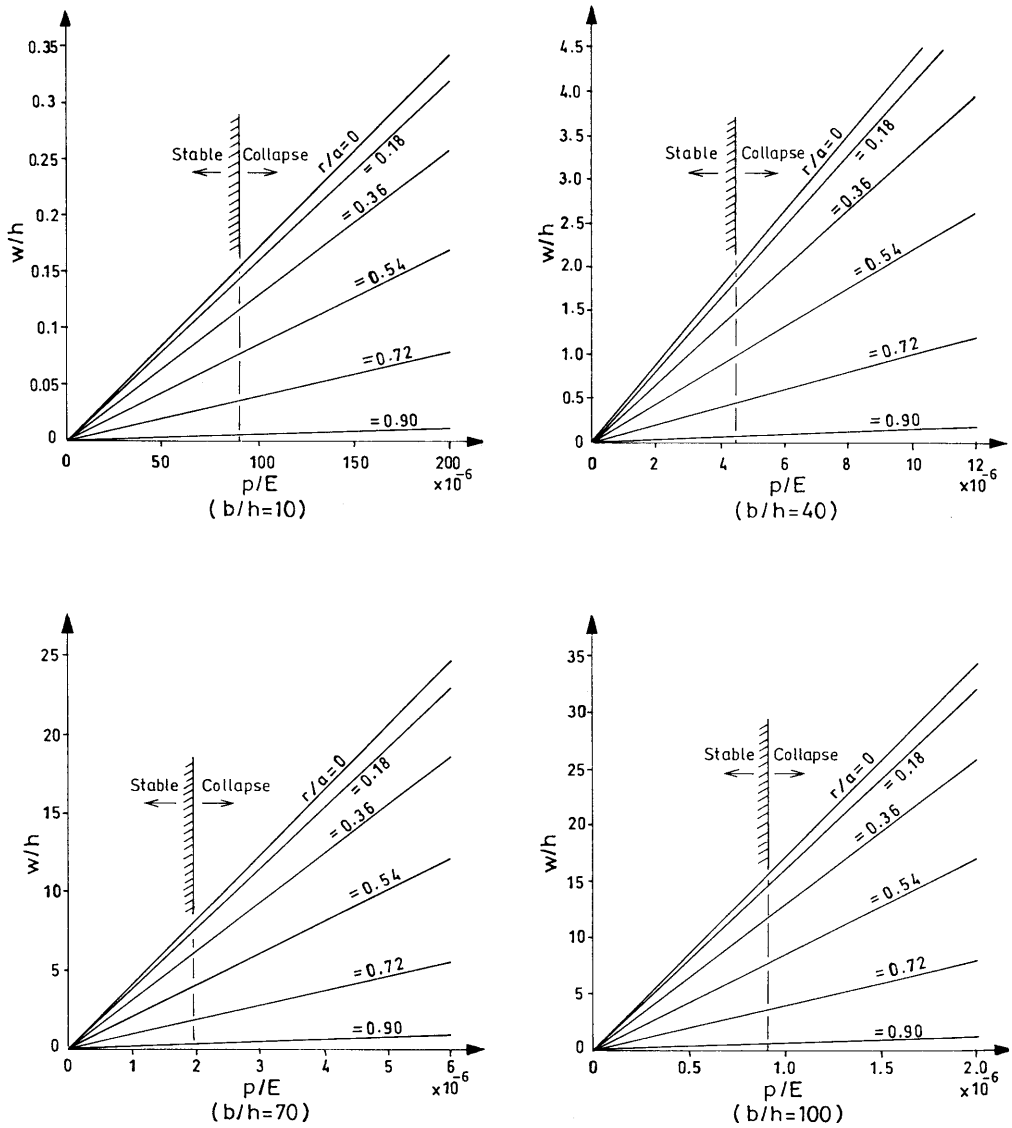

Fig. 11. Lateral deformation vs. applied pressure for clamped-edge plates.

3.3 Lateral Deformation

Lateral deformation of plates is obtainable from Eq. (19) for the clamped-edge case, and from Eq. (20) for the simply supported case. The deformation, in general, is dependent on the applied pressure, plate geometry (h,a) and material elastic properties (E,ν). The deformation, as given in Eqs (19) and (20), increases with increasing applied pressure until collapse is reached. The collapse pressure which limits the plate deformation can be determined non-dimensionally from Eqs (12) and (18) as:

$$\frac{P_c}{E} = \frac{3}{2}\left(\frac{Y}{E}\right)\left(\frac{h}{a}\right)^2$$

for simply supported plates (25a)

$$\frac{P_c}{E} = 3\left(\frac{Y}{E}\right)\left(\frac{h}{b}\right)^2$$

for clamped-edge plates (25b)

where the righthand sides of Eqs (25a) and (25b) are constant for a given thickness to radius ratio and known plate material. The Y/E ratio is a material constant which is approximately equal to 3×10^{-3} for most engineering materials. This value is adopted in this study.

The variation of lateral deformation throughout the plate, i.e. from centre to edge, is plotted in Figs 8 and 9 for increasing pressures and a given thickness to radius ratio. The curve at collapse is shown by hatching in each figure.

The lateral deformation versus applied pressure is also presented throughout the plate, and the results are presented in Fig. 10 for simply supported plates and in Fig. 11 for clamped-edge plates. The collapse pressure is also shown on both figures.

For excessive deformation, Eq. (21) should be used instead of Eq. (20) for calculating the lateral deformation at the vicinity of the plate centre ($r/a \cong 0$). The results are presented in Fig. 12 where the collapse pressure trajectory is shown for each

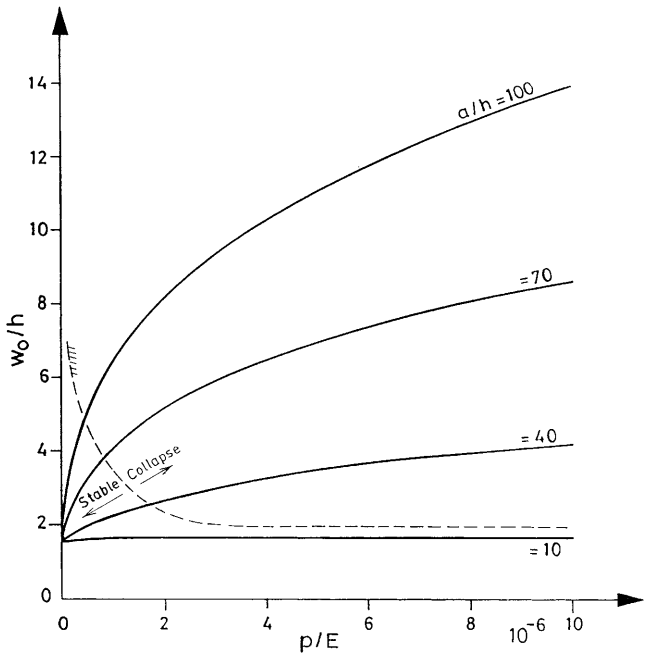

Fig. 12. Excessive central deformation of simply supported plates.

a/h value, which agrees well with the collapse pressure results in Fig. 10. However, the difference in results between the magnitudes of deformation given in Fig. 10 and those given in Fig. 12 is due to the fact that the results obtained in Fig. 10 are based on elastic analysis whereas those obtained in Fig. 12 are approximate and measured only at the onset of collapse, where the deformation keeps on increasing without or with little increase in the applied pressure.

4. Experimental Verification of Analytical Results

The criterion outlined in this study was verified using the experimental results given in [10] in which a total of 19 edge-clamped circular plates made of aluminium alloys, stainless steel and a magnesium alloy were tested under increasing normal hydraulic pressure. The centre deflection of the plates was measured in each case and plotted against the applied pressure. All tested plates were 127 mm (5 in) in diameter and had thicknesses ranging from 0.378 to 1.842 mm. For verification, it was decided to quote the experiments carried out on the three 24S – RT alclad aluminium plates (A, B and C) and compare the results given in [10] with those outlined in this study under similar loading conditions. The alclad aluminium alloy has a Young's modulus of elasticity of 71.66 GPa (10.4 × 10^6 p.s.i.), an average yield strength of 380.3 MPa (55.2 kips/in^2) and a Poisson's ratio of 0.3.

The superposition of the experimental and analytical results is shown in Fig. 13, which indicates a good correlation between them, with no more than a 12% deviation from the beginning of loading until the onset of collapse, for the three tested plates. Beyond collapse, the plates deform plastically and the analytical results begin to be greater than the experimental

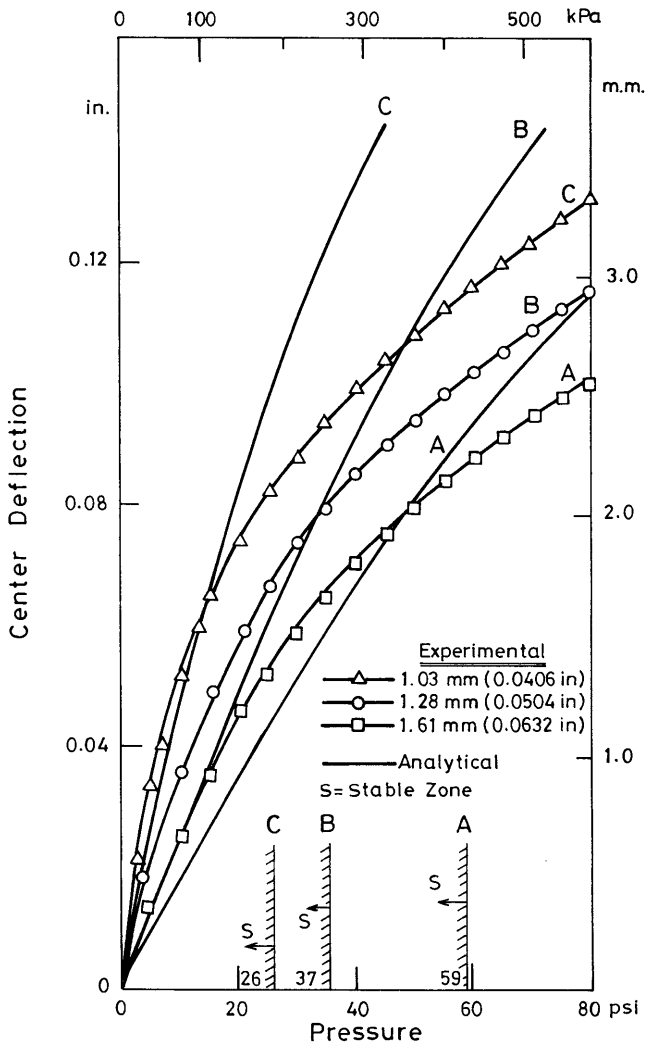

Fig. 13. Experimental and analytical results of 24S-RT alclad aluminium clamped plates subjected to normal pressure.

ones. This is mainly due to the fact that the plates become strain hardened during plastic deformation. The effect of strain hardening is not accounted for in the procedure of this study, which if accounted for could lead to even better correlation of the results. A study of this effect is planned. Nevertheless, we can say that the analytical and experimental results follow the same trend, and the procedure outlined in this study can be safely adopted for hydroforming applications that involve thin plates processed by lateral pressure.

5. Conclusions

The analysis carried out in this study helps to determine the bending moment, stress, and deformation distributions in a circular plate when processed by hydroforming. Collapse pressure, at which the plate material starts to undergo excessive deformation with little or no additional applied pressure, is also determined. The material is assumed to be elastic-perfectly

plastic with a negligible strain-hardening effect. The following conclusions are obtained from the results presented in the study.

1. The distributions of bending moments, stresses, and deformation, together with zones where these values reach maxima, are obtained using the principles of strength of materials. These maximum values occur near the centre of the plate, and, consequently, it is anticipated that maximum reduction of plate thickness that leads to rupture will also occur near the centre.
2. Clamping the plate during hydroforming helps to limit the lateral deflection and increase the pressure at collapse.
3. Collapse pressure was found to depend mainly on the plate edge conditions, its thickness to radius ratio and the material elastic properties. The collapse pressure is defined in this study as the pressure at which excessive deformation is obtained with or without little increase in the applied pressure.
4. Plate deformation increases with increasing applied pressure, but is restricted by collapse and tends to be less if the edges are clamped.

Acknowledgements

This project is sponsored by the Research Administration of Kuwait University under Grant no. EM-128. Moreover, the authors wish to thank Mr A. Shaheen for making the art work of the project and Ms A. Noronha for preparing the art work of the manuscript.

References

1. C.-M. Ni, "Stamping and hydroforming process simulations with a 3D finite element code", SAE Technical Paper 940753, 1994.
2. M. Mason, "Hydroform tubes for automotive body structure applications", SAE Technical Paper 930575, 1993.
3. "Hydroforming technology", Advances in Materials and Processes, pp. 50–53, May 1997.
4. S. D. Liu, D. Meuleman and K. Thompson, "Analytical and experimental examination of tubular hydroforming limits", SAE Technical Paper 980449, 1998.
5. S. Yossifon and J. Tirosh, "On the permissible fluid-pressure path in hydroforming deep drawing processes-analysis of failures and experiments", Transactions ASME Journal of Engineering for Industry, 110, pp. 146–152, May 1988.
6. R. D. Cook and W. C. Young, Advanced Mechanics of Materials, 2nd edn, pp. 379–410, Prentice-Hall, 1999.
7. W. C. Young, Roark's Formulas for Stress and Strain, 6th edn, McGraw-Hill, New York, 1989.
8. H. L. Langhaar, Energy Methods in Applied Mechanics, John Wiley, New York, 1962.
9. S. Timoshenko and S. Woinowsky-Krieger, "Theory of Plates and Shells", 2nd edn, McGraw-Hill, New York, 1959.
10. A. E. McPherson, W. Ramberg and S. Levy, "Normal pressure tests of circular plates with clamped edges", NACA Report 744, 1975.

Nomenclature

a	circular plate radius
E	Young's modulus of elasticity
h	plate thickness
M_o	bending moment upper limit
M_r	bending moment in radial direction per unit length
M_θ	bending moment in tangential direction per unit length
p	transverse load per unit area of plate
p_c	collapse pressure
Q_r	shearing stress
r,θ	polar coordinates
Y	yield strength of material in simple tension
σ_r	radial stress
σ_θ	tangential stress
ν	Poisson's ratio
w	plate lateral deflection
w_o	plate lateral deflection at its centre